World Conference on Timber Engineering Oslo 2023

COMPRESSIVE STIFFNESS PARALLEL TO GRAIN IN TIMBER

Marina Totsuka[1], Robert Jockwer[2], Kenji Aoki[3], Masahiro Inayama[4]

ABSTRACT: This paper describes results and analysis of experiments of compressive stiffness parallel to grain of glulam, with the focus on the damage zones near loading plates and joints. To investigate the influence factors of physical properties and the mechanism of the damage zone near the loading plates or the joints, compression tests on 90 specimens were performed. As a result, it was observed that damage zones exist near the loading plates and the joints. The Young's modulus of the damage zone was approximately 2% of that of a common longitudinal modulus of elasticity. The lengths of the damage zone of wood-wood joints are larger than that of wood-steel joints. The length of the damage zone and its scatter increase as the width of the cross-section increases. In the specimens, the lengths of the damage zone were 0.7~4.7mm. Therefore, the length of the damage zone has a size effect of the cross-sectional area and depends on the processing accuracy on the contact surface. The size effect was evaluated by the strongest link model and the evaluation method of the compressive stiffness parallel to the grain was proposed.

KEYWORDS: Glulam, Damage zone, Compression parallel to grain, Joints, Connections, Timber

1 INTRODUCTION

In connections of timber buildings, the deformations under compression parallel to the grain are often ignored since the deformations under compression perpendicular to the grain are bigger than the deformations under compression parallel to the grain due to the anisotropy of wood. However, in high-rise timber buildings, we may need to consider the deformation under compression parallel to the grain as well [1].

The heterogeneity of the strains in members loaded in compression parallel to the grain of clear specimens was reported in papers [2, 3] (Choi et al. and Dahl and Malo). In compression parallel to the grain, it is observed that the largest strains are allocated near the loading plates [4] (Zink et al.), which create a zone often called the "damage zone" as shown in Fig. 1. The zone between these damage zones is referred to as the "middle zone". Xavier et al. [5] and Brabec et al. [6] investigated the behaviour of the damage zones, e.g. the length and the modulus of elasticity, in small clear specimens. In addition, Totsuka et al. [7] reported the heterogeneity of the strains of large-sawn-timber specimens and showed the possibility that the length of the damage zone increases with increasing widths of the loaded area and the length of the damage zone does not change when the full height of the specimens increases. However, there is no evaluation method of the damage zone and the behaviour of the damage zones in glulam specimens remains unsolved so far.

In this present work, the compressive stiffness parallel to the grain of glulam was investigated. The aims of this work are as follows:

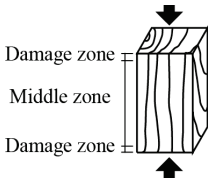

Figure 1: *Explanation of damage zone and middle zone*

(1) to clarify the influence factors of physical properties in the damage zone.
(2) to propose an evaluation method of compressive stiffness parallel to the grain.

2 EXPERIMENTAL WORK [8]

2.1 SPECIMENS AND TEST METHODS

Table 1 shows an overview of the test series of glulam specimens. The specimens were made from glulam of Norway Spruce (*Picea abies*) of quality GL30h according to SS-EN 14080:2013 [9], and Japanese cedar (*Cryptomeria japonica*) of quality E65-F255 and Japanese cypress (*Chamaecyparis obtusa*) of quality E95-F315 according to JAS (Japanese Agricultural Standards) [10]. The thickness of the glulam laminae was 42 mm for Norway Spruce and 30 mm for Japanese cedar and Japanese cypress. The width of the glulam laminae was the same as the specimen width. A total of 90 specimens were prepared by manufacturing 6 or 4 specimens per series. The test parameters are the size of the specimens and the type of joints (Fig.2). The specimens of series 20-3sSp had a 9mm steel plate. The specimens had typical wood characteristics, adhesive layers, and finger joints, however, the specimens of series 2.5-1Sp, 2.5-1Ce, and

[1] Marina Totsuka, Chiba University, Japan, mtotsuka@chiba-u.jp
[2] Robert Jockwer, Chalmers University of Technology, Sweden, robert.jockwer@chalmers.se
[3] Kenji Aoki, The University of Tokyo, Japan, aoken@g.ecc.u-tokyo.ac.jp
[4] Masahiro Inayama, The University of Tokyo, Japan, ainayama@g.ecc.u-tokyo.ac.jp

https://doi.org/10.52202/069179-0035

2.5-1Cy did not exhibit visual defects (knots and cracks) and did not have adhesive layers and finger joints.
The compression tests of the specimens were carried out with an in-line 3000 kN load cell and a spherically seated loading-head, an in-line displacement transducer under displacement control at a rate of 1 mm/min. The deformations and local strains were measured by the digital image correlation (DIC) system [11].

2.2 TEST RESULTS AND DISCUSSION

2.2.1 Compressive stiffness parallel to the grain

According to the equilibrium and linear elastic constitutive equations, the following closed-form solution can be obtained for the identification of the longitudinal modulus of elasticity:

Table 1: *Test series.*

Series	Species	#	Specimen size [mm]		Joint type
			A	*H*	
2.5-1Sp	Norway spruce	6	25×25	100	-
10-1Sp			100×100	100	-
20-1Sp			200×200	100	-
20-05Sp			200×200	50	-
20-3Sp			200×200	300	-
20-3bSp		4	200×200	300	Butt(Parallel)
20-3bxSp			200×200	300	Butt(Cross)
20-3sSp			200×200	300	Steel plate
2.5-1Ce	Japanese cedar	6	25×25	100	-
10-1Ce			100×100	100	-
20-1Ce			200×200	100	-
20-2Ce			200×200	200	-
2.5-1Cy	Japanese cypress	6	25×25	100	-
10-1Cy			100×100	100	-
20-1Cy			200×200	100	-
20-2Cy			200×200	200	-

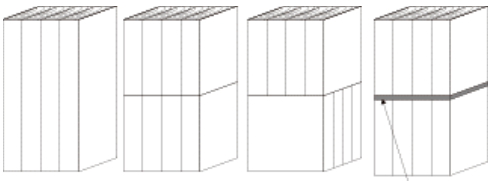

Table 2: *Mean statistics of specimens*

	Longitudinal modulus of elasticity in full height $E_{L,f}$ [N/mm²]							
Mean	4383	4432	5349	6649	6823	6284	8242	10091
CV [%]	19	5	4	1	20	6	5	4
	Longitudinal modulus of elasticity in middle zone $E_{L,m}$ [N/mm²]							
Mean	7549	8807	14318	9722	14966	15247	22575	14847
CV [%]	12	14	34	8	11	15	18	8

	Longitudinal modulus of elasticity in full height $E_{L,f}$ [N/mm²]							
Mean	5327	4920	2507	1601	5510	2558	2381	2670
CV [%]	9	11	3	7	4	3	6	2
	Longitudinal modulus of elasticity in middle zone $E_{L,m}$ [N/mm²]							
Mean	13155	12440	13950	13414	11865	13240	12500	14064
CV [%]	13	9	16	18	5	9	10	11

Note: CV is coefficient of variation.

$$E_{\mathrm{L}} = \frac{P}{A\varepsilon_1} \quad (1)$$

Where P is the applied compression load, A is the cross-sectional area (the loaded area), and ε_1 is the linear strain, from $0.2P_{max}$ to $0.4\ P_{max}$, along the longitudinal direction. In this study, two types of the E_L were calculated:
(1) the longitudinal modulus of elasticity in full height ($E_{L,f}$) using the ε_1 by the displacement transducers,
(2) the longitudinal modulus of elasticity in the middle zone ($E_{L,m}$) using the ε_1 in the middle zone measured by the DIC.
Table 2 shows the statistics of the specimens. The values of $E_{L,m,}$ were independent of the dimensions (height and width) of the specimens and the joint types. The mean values of $E_{L,m}$ were close to the literature values (7350 N/mm² for cedar and 11700 N/mm² for spruce[12], but no literature value for cypress) and considered to be equivalent to Young's modulus measured with a strain gauge or displacement meter attached to the middle of the test specimen. The mean values of $E_{L,m}$ of series 20-1Ce and 20-1Cy were bigger than those of the other series. The reason for this is unknown and further consideration will be needed to yield any findings about it.
Fig. 3 presents the influence of the heights and the widths of the loaded area on the values of $E_{L,f}$. The test results of solid timber of cedar [7] are also shown in Fig. 3 These values indicate mean values of the specimens with a cross-sectional area of 200×200 mm and 30×30 - 90×90 mm [7] for the influence of the heights and with a height of 100 mm and 30 - 90 mm [7] for the influence of the widths of the loaded area. The $E_{L,f}$ had an increasing trend as the height increased. This can be explained by the fact that the lengths of the damage zone do not change when the full height of the specimens increases. The $E_{L,f}$ had an increasing trend as the width of the loaded area decreased in the spruce-specimens and solid timber. This can be explained by the increasing lengths of the damage zone with the increase of the widths of the loaded area. However, the $E_{L,f}$ did not have an increasing trend in the cedar- and cypress-specimens. To clarify the mechanism of the damage zone, the damage zones were analysed in the following.

2.2.2 Strain field characterization and length of the damage zone

Fig. 4 shows an example of the deformation field of the longitudinal strain at 20% and 40% of the maximum load (P_{max}) of the series 10-1Sp by DIC. A damage zone near the loading plates or the joints and the middle zone can be recognized. The strain in the damage zone had a gradual distribution along with the height and exponentially increase as the distance from the loading plate or the joint

decreased. The phenomenon of the damage zone near the loading plates is in agreement with the observations made by Brabec [6]. The maximum strain is dependent on the load, but the length of the damage zone at 20% of the P_{max} was almost the same as that at 40% of the P_{max}.

Fig. 5 shows the longitudinal strain curves at 20% of the P_{max} of the specimens by DIC. The length of the damage zone seemed to be independent of the height, but the length of the damage zone increases as the loaded area increases. A detailed discussion of the length of the damage zone is provided in Fig.6-8. Fig. 5 (f)(g)(h) shows the longitudinal strain curves of wood-wood joints and wood-steel joints. The damage zones were also observed near the wood-wood joints and wood-steel joints, as well as near the loading plates.

Where the damage zone was defined at a strain ε_1 of -0.2% and less at 20% of P_{max}, the average lengths of the damage zone were 0.9 mm in 2.5-1Ce, 0.7 mm in 2.5-1Cy, 1.1 mm in 2.5-1Sp, 0.7 mm in 10-1Ce, 0.9 mm in 10-1Cy, 2.3 mm in 10-1Sp, 1.3 mm of the cedar- specimens with 200 mm, 1.0 mm of the cypress-specimens with 200 mm, and 4.7 mm of the spruce specimens with 200 mm width. Positive correlations were suggested between the length of damage zone and the width of the cross-section with correlation coefficients of +0.52 for the cedar-specimens, +0.41 for the cypress-specimens and +0.81 for the spruce-specimens. The length of the damage zone and its scatter increase as the width of the cross-section increases. This trend was especially remarkable in the spruce specimens. It was probably because the spruce specimens were processed on a different machine and the processing of the spruce specimens was rougher than that of the cedar- and cypress-specimens. The cedar- and cypress-specimens were processed on the same machine. The surface roughness of the contacted area is likely to increase as the cross-sectional area of the specimens increase. In other words, the length of the damage zone may depend on the accuracy of the processing machine. On the other hand, lower or negligible correlations between the length of the damage zone and the height of the specimen were indicated with correlation coefficients of +0.24 for the cedar-specimens, +0.46 for the cypress-specimens and +0.17 for the spruce-specimens in Fig.7. The length of the

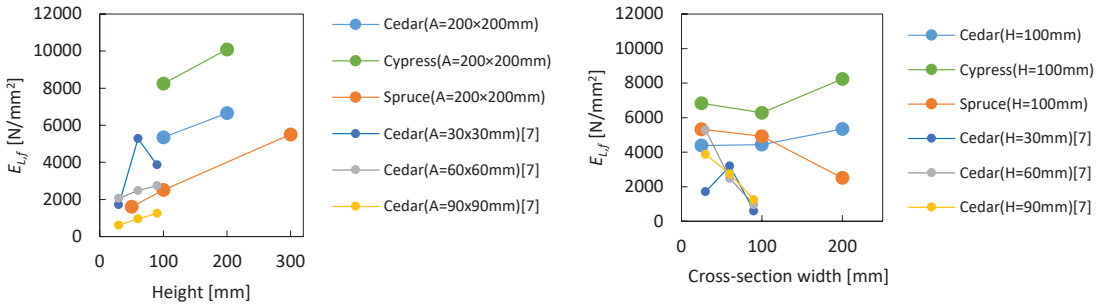

(a)Height vs. $E_{L,f}$ (b)Cross-section width vs. $E_{L,f}$

Figure 3: *Influence of heights and widths of cross-sectional area on values of EL,f .*

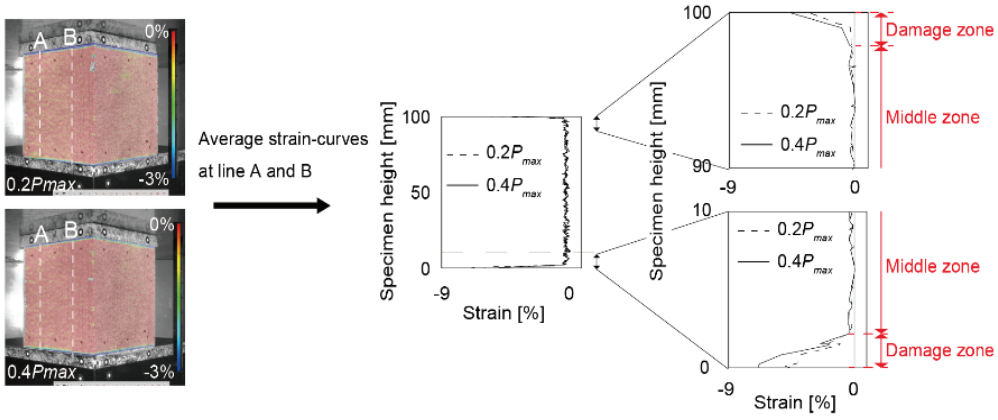

(a) Deformation fields of longitudinal strain (b) Average of the line A and B of 0.2 and 0.4 P_{max}

Figure 4*: Longitudinal strains of specimen 10-1Ce at 0.2 and 0.4 Pmax by DIC*

https://doi.org/10.52202/069179-0035

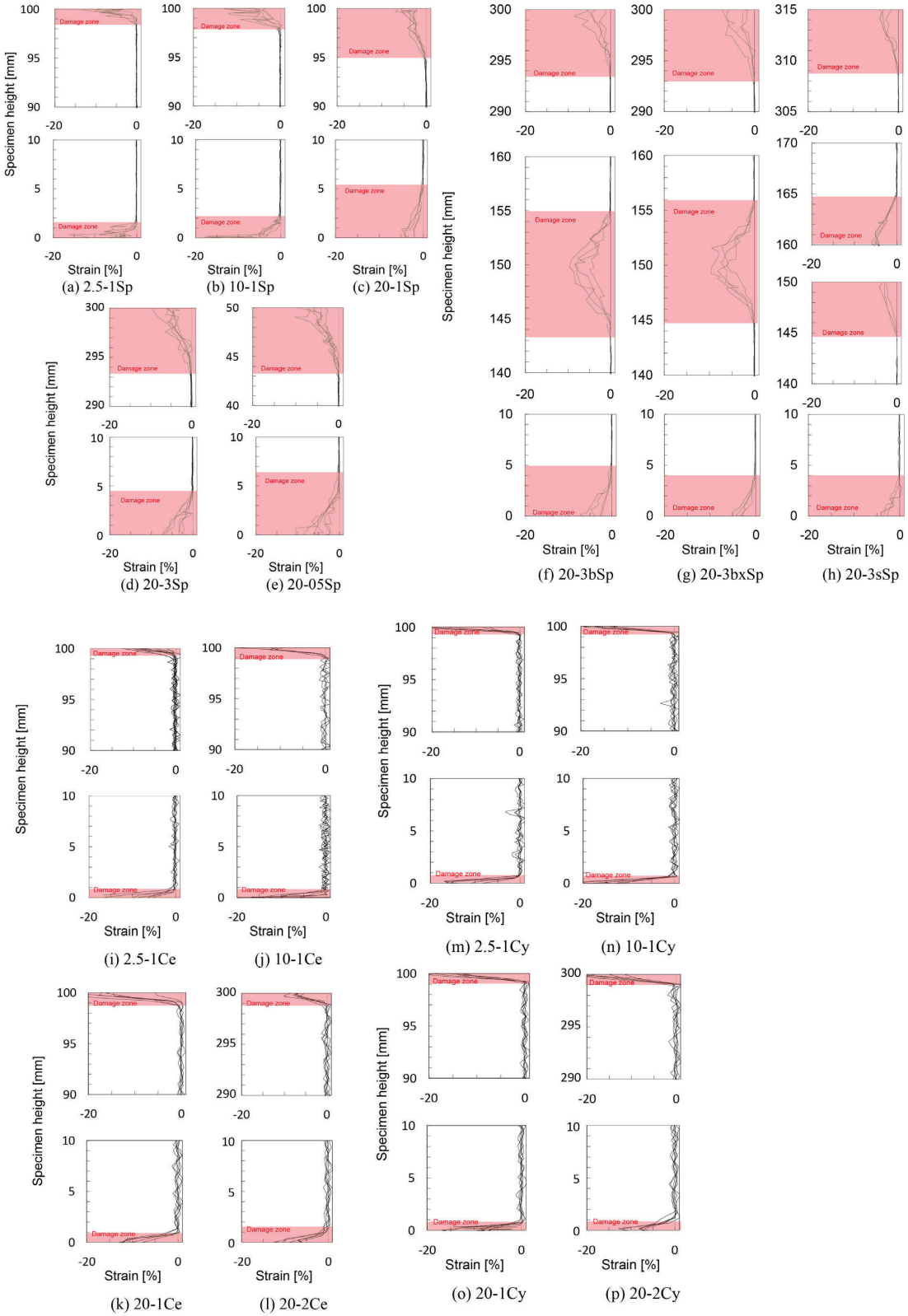

Figure 5: *Longitudinal strains distribution of specimens near loading plates in 0.2 Pmax*

damage zone did not change when the height of the specimen changed.

Fig.8 shows the length of the damage zone near wood-wood joints and wood-steel joints. It was considered that the lengths of the damage zone of wood-wood joints are larger than that of wood-steel joints.

3 EVALUATION METHOD OF COMPRESSIVE STIFFNESS

3.1 MODEL OF DEFORMATION DUE TO COMPRESSION PARALLEL TO GRAIN

A simple analytical spring model is used to evaluate the deformation of a specimen compressed parallel to the grain as shown in Fig. 9. If the Young's modulus is assumed to be constant in the damage zone, the specimen is modelled by two types of springs, and the stiffness at full height, K_f, is expressed by the following equations:

$$K_f = \frac{1}{\frac{2}{K_d} + \frac{1}{K_m}} = \frac{1}{\frac{2x}{0.02E_{L,m}A} + \frac{H-2x}{E_{L,m}A}} \quad (2)$$

where $E_{L.m}$ is the Young's modulus in the middle zone; A is the loaded area; H is the full height of the specimen; and x is the damage zone length.

In the previous study, Totsuka et al. [7] indicated that spreading effects in the compression parallel to the grain are small enough to be ignored for compressive stiffness. Therefore, the stiffness of specimens of partial compression are evaluated as the stiffness of specimens without margins.

3.2 DAMAGE ZONE LENGTH

The damage zone was considered to occur on the cut RT surface as shown in Fig. 10. The strongest link model was used to evaluate that the damage zone length and its scatter increased as the loaded area increased. The strongest link model [13] is the opposite of the weakest link model [14], in which a certain property (in this study, the damage zone length) is determined by the strongest (longest) element, as shown in Fig. 11. The probability $\boldsymbol{F_x}(x)$ that the length y of an element in a unit area is less than or equal to the length x is assumed to be a two-parameter Weibull distribution with the following equation:

$$\boldsymbol{F_x}(x) = 1 - e^{-\left(\frac{x}{x_0}\right)^m}, \quad (3)$$

where x_0 and m are the material parameters that define the magnitude and scatter in strength. In the model shown in Fig. 11, if all element lengths y are less than or equal to length x, the damage zone length is x. Therefore, when there are n elements, the probability $\boldsymbol{F_x}(x)$ that all element lengths y are less than or equal to x is expressed by the cumulative distribution function, given by the following equation:

$$\boldsymbol{F_x}(x) = \left(1 - e^{-\left(\frac{x}{x_0}\right)^m}\right)^n \quad (4)$$

For a specimen of a loaded area A, n can be replaced by A. Therefore, the probability $\boldsymbol{F_x}(x)$ is expressed by the following equation:

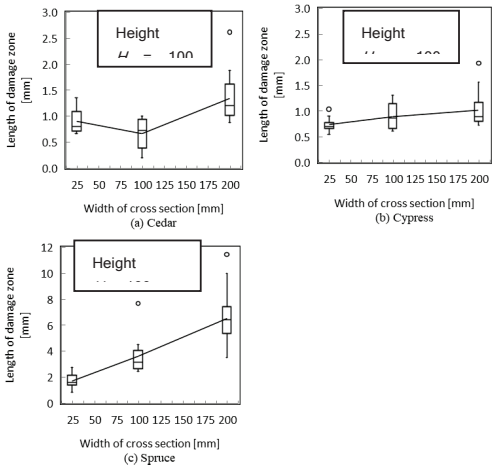

Figure 6: *Length of damage zone of specimens of varying widths of cross-section*

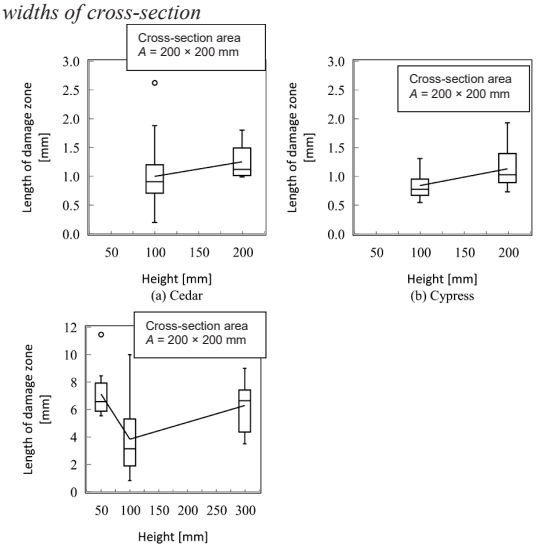

Figure 7: *Length of damage zone of specimens of varying heights*

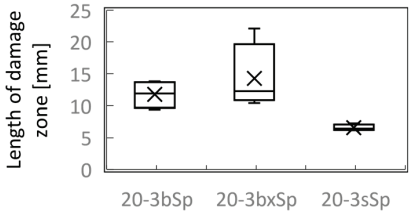

Figure 8: *Length of damage zone of specimens with wood-wood joints and wood-steel joints.*

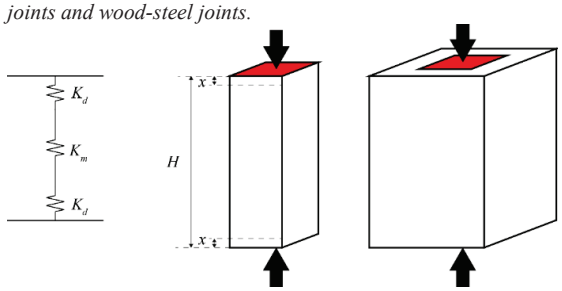

Figure 9: *Spring model of specimen compressed parallel to grain.*

https://doi.org/10.52202/069179-0035

$$\boldsymbol{F_x}(x) = \left(1 - e^{-\left(\frac{x}{x_0}\right)^m}\right)^A \quad (5)$$

Fig. 12 shows the cumulative probability distribution of the damage zone length obtained from the experiments and Eq. 5 with the material parameters, which are close to the experimental value. The solid line in the figure represents the experimental value, and the dashed line represents Eq. 5. The cumulative probability distributions of the experimental results can be successfully represented by the distributions of the strongest link model in Eq. 5, although the agreement was not perfect owing to the small number of specimens. Therefore, the size effect on the damage zone length can be explained by the strongest link model using the Weibull distribution.

In the strongest link model, the relationship between the damage zone lengths with loaded areas A_1 and A_2 can be as follows:

$$\boldsymbol{F_x}(x)^{\frac{1}{A}} = 1 - e^{-\left(\frac{x}{x_0}\right)^m} \quad (6)$$

$$1 - \boldsymbol{F_x}(x)^{\frac{1}{A}} = e^{-\left(\frac{x}{x_0}\right)^m} \quad (7)$$

$$\ln\left(1 - \boldsymbol{F_x}(x)^{\frac{1}{A}}\right) = -\left(\frac{x}{x_0}\right)^m \quad (8)$$

$$\left(-\ln\left(1 - \boldsymbol{F_x}(x)^{\frac{1}{A}}\right)\right)^{\frac{1}{m}} = \frac{x}{x_0} \quad (9)$$

If m, x_0, and $\boldsymbol{F_x}(x)$ are equal in the loaded areas A_1 and A_2, the relationship between the damage zone lengths x_1 and x_2 of the specimen with loaded areas A_1 and A_2 is as follows:

$$\frac{x_1}{x_2} = \left(\frac{\ln\left(1 - \boldsymbol{F_x}(x)^{\frac{1}{A_1}}\right)}{\ln\left(1 - \boldsymbol{F_x}(x)^{\frac{1}{A_2}}\right)}\right)^{\frac{1}{m}} = \left(\frac{\ln\left(1 - \boldsymbol{F_x}(x)^{\frac{1}{A_1}}\right)}{\ln\left(1 - \boldsymbol{F_x}(x)^{\frac{1}{A_2}}\right)}\right)^{k} \quad (10)$$

Where k is the size effect parameter. Fig. 13 shows the experimental results and approximate curves for Eq. 10 with the test of a 25 mm square section as the benchmark specimen (x_2 and A_2) when the cumulative probability is 50%. The size effect parameter k was 0.62 for cedar, 0.42 for cypress, and 3.12 for spruce specimens. The size effect parameter k of the strongest link model was similar to that of the weakest link model, indicating that the larger the parameter k, the larger the size effect.

Figure 10: *Photo of cut RT surface.*

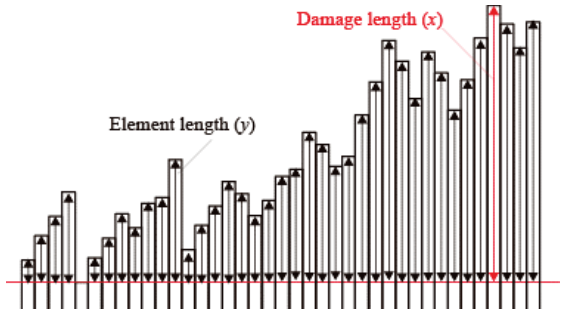

Figure 11: *Strongest link model of length of damage zone.*

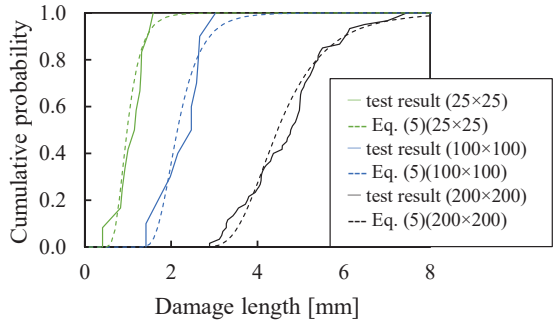

(a) Cumulative probability distribution of the damage zone length (Spruce)

Cross-sectional area [mm²]	25×25	100×100	200×200
A	625.00	10000	40000
x_0	0.05	0.05	0.05
m	0.479	0.601	0.645

(b) Material parameters (Spruce).

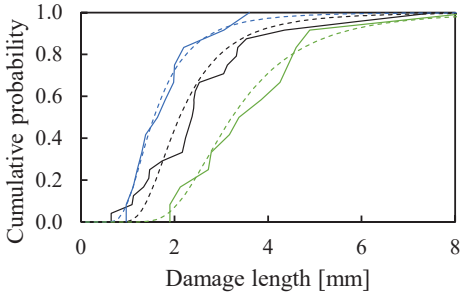

(c) Cumulative probability distribution of the damage zone length (Cedar)

Cross-sectional area [mm²]	25×25	100×100	200×200
A	625.00	10000	40000
x_0	0.0005	0.001	0.05
m	0.287	0.307	0.460

(d) material parameters (Cedar)

https://doi.org/10.52202/069179-0035

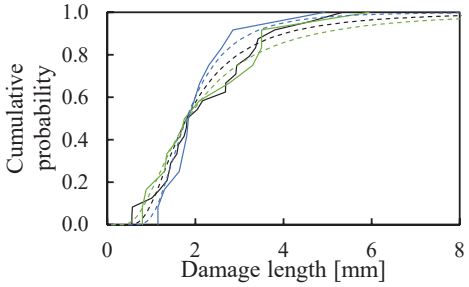

(e) Cumulative probability distribution of the damage zone length (Cypress)

Cross-sectional area [mm²]	25×25	100×100	200×200
A	625.00	10000	40000
x_0	0.001	0.001	0.00001
m	0.255	0.301	0.198

(f) material parameters (Cypress)

Figure 12: *Comparison of cumulative probability distribution of experimental result and Eq. 5.*

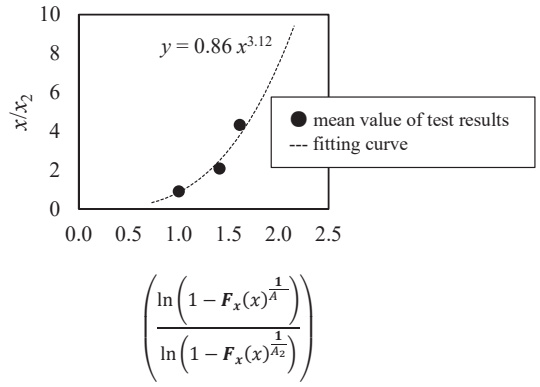

(a) Spruce specimens

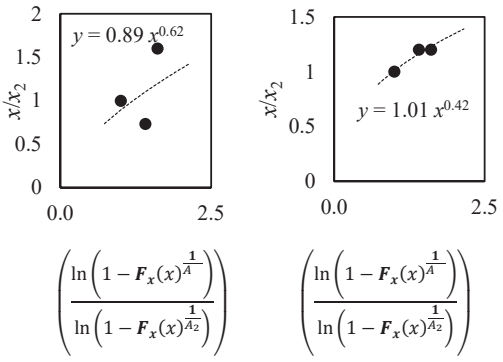

(b) Cedar specimens (c) Cypress specimens

Figure 13: *Experimental results and approximate curves for Eq. 10 when the cumulative probability is 50%.*

3.3 YOUNG'S MODULUS OF DAMAGE ZONE

The experimental value of the Young's modulus of the damage zone in Table 3 was calculated using Eq. 2 with the experimental data (mean value) in Table 2. The Young's modulus of the damage zone was 128-464 N/mm² for the spruce, 61-574 N/mm² for the cedar, and 98-491 N/mm² for the cypress specimens. The Young's modulus of the damage zone was higher for Japanese cypress than for cedar, even though the two specimens were processed by the same machine. Fig. 14 shows the ratio of the Young's modulus of the damage zone to the Young's modulus of the middle zone. No correlation was found between this ratio and wood species or dimensions of the specimen. The mean values of the Young's modulus ratios were 2.1% for the spruce, 2.4% for the cedar, and 1.5% for the cypress specimens, respectively. Therefore, the Young's modulus of the damage zone is considered to be approximately 2% of the Young's modulus of the middle zone.

Table 3: *Young's modulus of the damage zone*

Series [8]	Mean [N/mm²]	CV [%]
2.5-1Sp	197	19.0
10-1Sp	350	14.0
20-1Sp	293	8.33
20-05Sp	349	19.0
20-3Sp	304	16.2
20-3bSp	186	15.7
20-3bxSp	185	10.7
20-3sSp	196	13.0
2.5-1Ce	208	39.9
10-1Ce	118	38.3
20-1Ce	290	48.5
20-2Ce	270	27.4
2.5-1Cy	193	37.1
10-1Cy	192	22.9
20-1Cy	236	17.0
20-2Cy	359	21.2

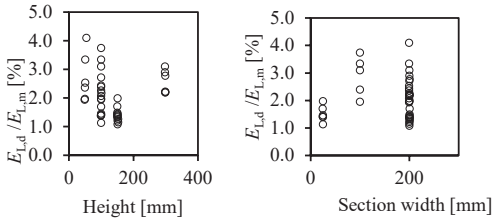

(a) Spruce specimens

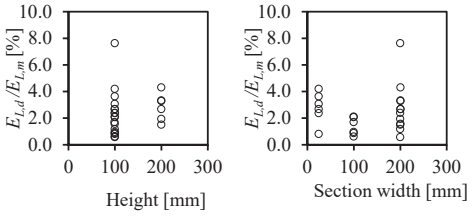

(b) Cedar specimens

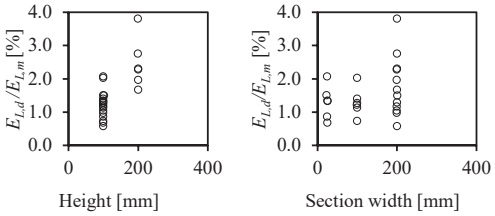

(c) Cypress specimens

Figure 14: Ratio of Young's modulus of damage zone to Young's modulus of the middle zone.

https://doi.org/10.52202/069179-0035

3.4 EXPERIMENTAL RESULTS AND CALCULATED RESULTS

The stiffness of the compression parallel to the grain can be evaluated using the following equations:

$$K_f = \frac{1}{\frac{2}{K_d} + \frac{1}{K_m}} = \frac{1}{\frac{2x}{0.02E_{L,m}A} + \frac{H-2x}{E_{L,m}A}} \quad (11)$$

$$x = \left(\frac{\ln\left(1 - \boldsymbol{F_x}(x)^{\frac{1}{A}}\right)}{\ln\left(1 - \boldsymbol{F_x}(x)^{\frac{1}{A_s}}\right)} \right)^{k} x_s \quad (12)$$

To shorten x, the size effect parameter should be small, and machining that does not increase the surface roughness significantly is recommended. Since a specimen with a smaller loaded area is less susceptible to the effects of machining accuracy, it is recommended that the benchmark specimen have a loaded area as small as possible (in this study, an ASTM 143 specimen, R25×T25×L100 mm, was used). The cumulative probability should be set to 50%, considering that the mean value is typically used as the stiffness of the joint in timber buildings. If the loaded area of the benchmark specimen is 25 mm square and the cumulative probability is 50%, Eq. 12 becomes:

$$x = \left(\frac{\ln\left(1 - 0.5^{\frac{1}{A}}\right)}{-6.8} \right)^{k} x_s \quad (13)$$

Fig. 15 shows the value calculated using Eq. 11 and 13 along with the experimental values of the stiffness K_f. The parameters k and x_s inserted in Eq. 13 were 3.12 and 0.86 for spruce specimens, 0.62 and 0.89 for cedar specimens, and 0.42 and 1.01 for cypress specimens, as shown in Fig. 13. The calculated values are considered to be satisfactorily close to the experimental values.

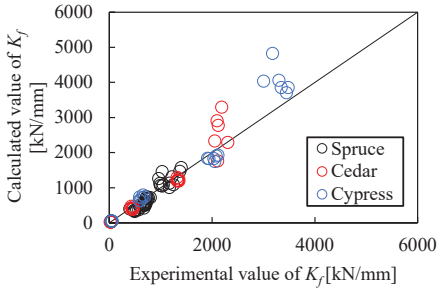

Figure 15: *Calculated value and experimental value of compressive stiffness parallel to the grain*

4 CONCLUSIONS

The properties of the damage zone of timber compressed parallel to the grain were studied using experimental results and computational models. The damage zone length and its scatter increased as the loaded area increased. No correlation was found between the ratio of the Young's modulus of the damage zone to the Young's modulus of the middle zone and the wood species or dimensions. The Young's modulus of the damage zone was approximately 2% of that of the middle zone. In addition, an evaluation method for the damage zone length is proposed using the strongest link model to consider the size effect of the damage zone length. The Young's modulus and damage zone length evaluation methods obtained above were used to evaluate the stiffness of the specimens compressed parallel to the grain. The proposed method could evaluate the experimental values reasonably well.

In the future, the proposed method for the damage zone can be applied to a variety of timber connections.

ACKNOWLEDGEMENT

This work was supported by a Grant-in-Aid for JSPS Research Fellows Number JP19J13253 and Grant-in-Aid for Young Scientists(Start-up) 21K204583.

REFERENCES

[1] M. Totsuka, J. Hayakawa, K. Aoki, M. Inayama (2022) Evaluation of stiffness parallel to grain of wood based on strongest link model, Journal of Structural and Construction Engineering (Transactions of AIJ),87(798): 770-779, doi.org/10.3130/aijs.87.770.

[2] Choi D, Thorpe JL, Hanna RB (1991) Image analysis to measure strain in wood and paper. Wood Sci Technol 25:251–262. doi. org/ 10. 1007/BF002 25465

[3] Dahl KB, Malo KA (2009) Planar strain measurements on wood specimens. Exp Mech 49:575–586. doi. org/ 10. 1007/ s11340-008- 9162-0

[4] A.G. Zink, R.W. Davidson, R.B. Hanna (1995) Strain measurement in wood using a digital image correlation technique, *Wood Fiber Sci.* 27 346–359.

[5] J. Xavier, A.M.P. de Jesus, J.J.L. Morais, J.M.T. Pinto (2012) Stereovision measurements on evaluating the modulus of elasticity of wood by compression tests parallel to the grain, *Constr. Build. Mater.* 26 207–215.doi.org:10.1016/j.conbuildmat.2011.06.012.

[6] M. Brabec, J. Tippner, V. Sebera, J. Milch, P. Rademacher, Standard and non-standard deformation behavior of European beech and Norway spruce during compression, *Holzforschung*. 69 1107–1116,2015. doi.org:10.1515/hf-2014-0231.

[7] M. Totsuka, R. Jockwer, K. Aoki, M. Inayama, Experimental study on partial compression parallel to grain of solid timber, *J. Wood Sci.* 67 2021. doi.org:10.1186/s10086-021-01972-w.

[8] Totsuka M, Jockwer R, Kawahara H, Aoki K, Inayama M (2022) Experimental study of compressive properties parallel to grain of glulam. J Wood Sci., 68:33. doi.org/10.1186/s10086-022-02040-7.

[9] SS-EN 14080 (2013) Timber structures—Glued laminated timber and glued solid timber—requirements. Swedish Institute for Standards. Stockholm.

[10] Japanese agricultural standards notice no. 1587 (2012) Glulam. Ministry of Agriculture. Forestry and Fisheries. Tokyo (In Japanese)

[11] GOM Correlate (GOM GmbH, Germany).

[12] Ringyo-shikenjo, (ed) (1958) Mokuzai kogyo handbook. Maruzen, Tokyo

[13] Gustafsson PJ, Jockwer R, Serrano E, Steiger R.(2015) A strongest link model applied to fracture propagating along grain. Proceedings of meeting 48. International network on timber engineering research. Timber Press Scientific, p. 351–66.

[14] Weibull W. (1939) A statistical theory of the strength of materials, R. Swedish Inst. J Eng Res. 151:1–45.